ACS OMEGA

Open Access



http://pubs.acs.org/journal/acsodf

Article

# Lonidamine Increases the Cytotoxic Effect of 1-[(4-Amino-2-methyl-5-pyrimidinyl)methyl]-3-(2-chloroethyl)-3-nitrosourea via Energy Inhibition, Disrupting Redox Homeostasis, and Downregulating MGMT Expression in Human Lung Cancer Cell Line

Tengjiao Fan,[#] Lin Shen,[#] Yaxin Huang, Xin Wang,* Lijiao Zhao, Rugang Zhong, Peng Wang,* and Guohui Sun*

Cite This: *ACS Omega* 2024, 9, 36134−36147

Read Online

ACCESS | Metrics & More | Article Recommendations | Supporting Information

**ABSTRACT:** Lung cancer ranks as the second most diagnosed cancer and the leading cause of cancer-related deaths worldwide. Novel chemotherapeutic strategies are crucial to efficiently target tumor cells while minimizing toxicity to normal cells. In this study, we proposed a combination strategy using energy blocker lonidamine (LND) and cytotoxic drug nimustine (ACNU, 1-[(4-amino-2-methyl-5-pyrimidinyl)-methyl]-3-(2-chloroethyl)-3-nitrosourea) to enhance the killing of a human lung cancer cell line and investigated the potential chemo-sensitizing mechanism of LND. LND was found to remarkably increase the cytotoxicity of ACNU to A549 and H1299 cells without significantly affecting normal lung BEAS2B cells. The combination of LND and ACNU also produced significant effects on cell apoptosis, colony formation, cell migration, and invasion assays compared to single drug treatment. Mechanistically, LND decreased intracellular ATP levels by inhibiting glycolysis and inducing mitochondrial dysfunction. Furthermore, the combination of LND and ACNU could intensify cellular oxidative stress, decrease cellular GSH contents, and increase reactive oxygen species (ROS) production. Notably, LND alone dramatically downregulated the expression of DNA repair protein MGMT ($O^6$-methylguanine-DNA methyltransferase), enhancing DNA interstrand cross-link formation induced by ACNU. Overall, LND represents a potential chemo-sensitizer to enhance ACNU therapy through energy inhibition, disrupting redox homeostasis and downregulating MGMT expression in human lung cancer cell line under preclinical and clinical background.

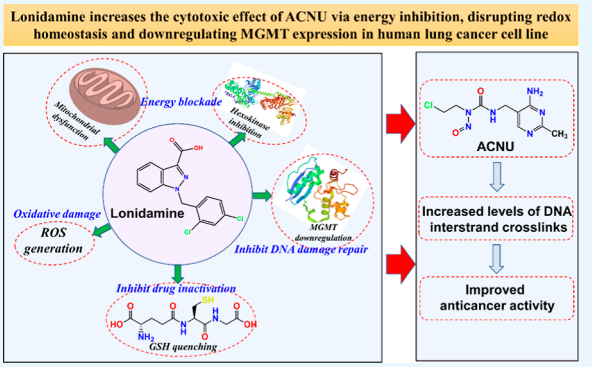


## 1. INTRODUCTION

According to the latest global cancer statistics, lung cancer is estimated as the second most diagnosed cancer (11.4%) and the leading cause (18%) of cancer mortality worldwide.[1] The metastatic characteristic and drug resistance make the treatment of lung cancer a great challenge, although several kinase inhibitors like gefitinib and dacomitinib have been approved for clinical application.[2] Usually, a monofunctional drug is very difficult to efficiently kill tumor cells because they commonly have multiple survival or resistance pathways.[3] In this case, combi-molecules or combination therapy targeting two or more cellular targets are promising for the treatment of malignant tumors.[3,4]

DNA antitumor alkylating agents, such as nimustine (ACNU), carmustine (BCNU), lomustine (CCNU), temozolomide (TMZ), and procarbazine (PCZ), are widely used in the cancer treatment, including brain tumor, lung cancer, leukemia, and Hodgkin's lymphoma.[5,6] ACNU, BCNU, and CCNU are bifunctional DNA alkylating agents, whose antitumor activity is mainly associated with the DNA interstrand cross-links (ICLs) between G and C.[5−8] The formation of DNA ICLs is the result of $O^6$-choloethylation of guanine.[5,6,8] TMZ and PCZ are monofunctional alkylating agents, which exert antitumor activity via the formation of $O^6$-methylguaine ($O^6$-MG).[9−11] However, tumor resistance seriously limits their clinical applications. For example, $O^6$-methylguanine-DNA methyltransferase (MGMT) can remove the alkyl groups located at the DNA guanine to the Cys145 residue of its active center, leading to the decrease in the level of $O^6$-MG or DNA ICLs.[9,12,13] MGMT is a frequently studied resistance target for improving the chemotherapeutic effects of such agents over the past several decades.[12−16] Up to date, $O^6$-benzylguanine ($O^6$−BG) and $O^6$-(4-bromothenyl)guanine

Received: January 19, 2024
Revised: July 30, 2024
Accepted: August 13, 2024
Published: August 17, 2024

(lomeguatrib, $O^6$-4-BTG) are two MGMT inhibitors entering clinical trials.[17,18] However, it is disappointing that the combination of the two MGMT inhibitors with the aforementioned guanine $O^6$-alkylating agents produced serious adverse effects in tumor patients as the chemo-sensitization was also observed in normal tissues.[12,13] As a matter of fact, ATP-dependent multidrug resistance (MDR) and GSH-mediated drug inactivation also result in the occurrence of tumor resistance.[19−22] Therefore, other pathways must be considered to overcome the resistance.

It is well-known that tumor cells have unique energy metabolism characteristics that are highly dependent on glycolysis rather than mitochondrial oxidative phosphorylation (OXPHOS) for energy supply.[23] The altered glucose metabolism is characterized by high glucose uptake and lactate production, and this metabolic reprogramming supports rapid cell growth and proliferation by providing both energy and biosynthetic precursors.[23−25] This unique metabolism is called "Warburg effect", which is associated with intrinsic or acquired resistance to radiotherapy and routine anticancer drugs via generating an extracellular acid microenvironment, a chemically reduction milieu, activating DNA damage repair and triggering exosome release.[26] In fact, tumor cell is a hybrid glycolysis/OXPHOS phenotype,[27] in which OXPHOS provides ∼40% energy, while glycolysis not only accounts for ∼60% energy but also supplies anabolic materials.[28] Therefore, it is highly suggested that blocking tumor energy metabolism may be a promising strategy to improve the therapeutic effects of conventional chemotherapeutic drugs. Indeed, several energy blockers like 3-bromopyruvate (3-BrPA), metformin, 2-deoxy-D-glucose (2-DG), and lonidamine (LND) have been used in combination therapy and exhibited promising results with respect to chemoresistance.[23,29−33] Among, LND has a special attention because of its initial usage as antispermatogenic drug.[34] In addition, as a single drug, LND has limited anticancer activity; however, it exhibits low toxicity to normal cells and high tumor selectivity.[29,35−37] In several published papers, LND selectively reduced the energy levels and intracellular pH of tumor cells while had no remarkable influence on normal tissues such as skeletal muscle and brain.[35,36] When LND is combined with conventional anticancer drugs such as nitrogen mustards,[36,38] doxorubicin,[39,40] and TMZ,[41] significant tumor growth inhibition has been reported.

The beneficial effects of LND for human heath provide a novel window in therapeutic intervention when in combination with other chemotherapeutic drugs. Recently, we reported an interesting study using the combination strategy of LND and ACNU in human glioblastoma cells in vitro and in vivo.[42] In this study, we investigated the sensitizing effects of LND on the anticancer activity of ACNU in the human lung cancer A549 cell line. ACNU was chosen in this study because it can be used for the treatment of lung cancer in a clinical setting. The underlying chemosensitizing mechanism mediated by the LND was also explored.

## 2. MATERIALS AND METHODS

**2.1. Chemicals.** LND and ACNU (hydrochloride) were purchased from Meryer Co., Ltd. (Shanghai, China) and TCI Co., Ltd. (Shanghai, China), respectively. *N*-acetylcysteine (NAC, Cat#A0737) were obtained from Aladdin Co., Ltd. (Shanghai, China). MEM-EBSS medium and penicillin−streptomycin were obtained from HyClone (South Logan, UT, USA). Fetal bovine serum (FBS) was purchased from Dakewe Biotech Co., Ltd. (Shenzhen, China). Trypsin with/without 0.25% ethylenediaminetetraacetic acid was purchased from GIBCO (Grand Island, USA) and ThermoFisher Scientific Inc. (Massachusetts, USA), respectively. 3-(4,5-Dimethylthiazol-2-yl)-2,5-diphenyltetrazolium bromide (MTT), dimethyl sulfoxide (DMSO), CellTiter-Lumi luminescent cell viability assay kit, reactive oxygen species (ROS) assay kit, enhanced BCA protein assay kit, phenylmethanesulfonyl fluoride (PMSF), sodium dodecyl sulfate-polyacrylamide gel electrophoresis (SDS-PAGE) gel quick preparation kit, loading buffer, and color protein ladder were obtained from Beyotime Biotechnology Co., Ltd. (Shanghai, China). Matrigel was purchased from Corning (New York, USA). GSH and lactic acid assay kits were obtained from Nanjing Jiancheng Bioengineering Institute (Nanjing, China). Crystal violet staining solution, hexokinase (HK) activity assay kit, mitochondrial membrane potential assay kit, and Hoechst 33342 solution were obtained from Beijing Solarbio Science & Technology Co., Ltd. (Beijing, China). The Annexin V-FITC/propidium iodide (PI) apoptosis detection kit was acquired from Yeasen (Shanghai, China). Mouse monoclonal $\beta$-actin monoclonal antibody was obtained from Proteintech Group, Inc. (Rosemont, USA). Goat antimouse IgG H&L 203 (IRDye 800CW), goat antirabbit IgG H&L (IRDye 800CW), rabbit monoclonal MMP2 primary antibody (ab181286), and rabbit monoclonal MGMT primary antibody (ab108630) were purchased from Abcam Inc. (Cambridge, UK). The DNA damage detection kit was obtained from KeyGEN BioTECH (Nanjing, China).

**2.2. Cell Culture.** Human nonsmall cell lung cancer (NSCLC) A549 and normal lung epithelial BEAS2B cell lines are gifts provided by Dr. Jingtao Li at Beijing University of Technology. Human NSCLC H1299 cell line was obtained from the Cell Resource Center, Peking Union Medical College. The tumor cells were maintained in MEM-EBSS (A549) or RPMI 1640 (H1299) or Dulbecco's modified Eagle's medium (BEAS2B) medium supplemented with 10% FBS, 100 U/mL penicillin, and 100 $\mu$g/mL streptomycin, respectively. The cells were cultured in a humidified incubator at 37 °C and 5% $CO_2$/95%. When reaching the confluence, cells were treated with drugs for the indicated time.

**2.3. Cytotoxicity Assay.** The MTT method was used to perform the cytotoxicity assay.[43] After seeding at 96-well plates and cultured for 24 h, the cells were incubated by LND or ACNU for 24 h or LND (24 h pretreatment) + ACNU (24 h treatment). After treatment, each well was added with 5 mg/mL MTT (20 $\mu$L) and allowed to incubate for 4 h in the dark. Subsequently, we added 150 $\mu$L of DMSO to completely solubilize formazan after removing the supernatant. The optical density (OD) at 570 nm was recorded using a Multiskan FC microplate reader (Thermo Scientific, Waltham, MA, USA). The mean cell viability was calculated as the percentage of the OD value of the control group. The survival rate (%) was calculated as $(OD_{drug} - OD_{blank})/(OD_{control} - OD_{blank}) \times 100\%$. For combination treatment, the $IC_{25}$ and $IC_{50}$ values of LND were used for 24 h pretreatment before exposure to ACNU. The synergy was calculated according to the following formula:[44] $Q = E_{(A+B)}/(E_A + E_B - E_A \times E_B)$, in which $Q < 0.85$ means antagonism, $Q = 0.85-1.15$ means additive, and $Q > 1.15$ means synergism. $E_{(A+B)}$ is the combined inhibition rate of LND and ACNU, and $E_A$ and


https://doi.org/10.1021/acsomega.4c00641
ACS Omega 2024, 9, 36134−36147

$E_B$ are the single inhibitory rates of drug A (LND) and B (ACNU), respectively.

**2.4. Colony Formation Assay.** Human NSCLC A549 cells (800 cells/well) were seeded at six-well plates. After 24 h of adherence, the cells were pretreated with LND for 24 h before treatment with ACNU (24 h). Each well was refreshed with fresh medium every 3 days. After a 9 day culture, the colonies were stained using 0.5% crystal violet, followed by a three time phosphate-buffered saline (PBS) washing. After the cells were dried at room temperature, the cloning number ($\geq$50 cells) was counted.

**2.5. Migration Assay.** The migration ability was assessed by a wound healing assay. Cells were seeded at six-well plates with appropriate density and cultured to ~90% confluence. A 10 $\mu$L pipet tip was used to make a scratch on the cell monolayer at the bottom of the six-well plate. The scraped cell debris was gently rinsed by PBS. Afterward, we added LND to the plate for a 24 h pretreatment, followed by treatment with ACNU for 48 h. The initial scratch width was expressed as $d_0$, and the width at different time points was also recorded. The migration rates at different time points were calculated based on the formula: Migration rate (%) = $(d_t - d_0)/d_0 \times 100\%$, among $d_t$ indicates the scratch width at $t$ h time point.

**2.6. Invasion Assay.** Briefly, after drug treatment, the cells were starved in a serum-free medium for 12 h. Subsequently, the cells were transferred to the upper side of the Matrigel-coated transwell insert (8 $\mu$m pore size) for 24 h incubation. The lower side of the transwell insert was filled with fresh medium containing 20% FBS to generate a concentration gradient. The cells were then stained with a 1% crystal violet solution for 40 min. After two times PBS washing, the transwell insert was taken for photographing after wiping the upper side cells using a cotton swab. The invading cells on the lower side were counted using ImageJ software (National Institutes of Health, USA).

**2.7. HK Activity Assay.** HK activity assay is based upon the reduction of $NADP^+$ to reduced nicotinamide adenine dinucleotide phosphate having maximum absorbance at 340 nm. After drug treatment, the cells were trypsinized, washed with PBS, and ultrasonically disrupted. Cell suspension was homogenized on ice, and the protein concentration was quantified by the BCA protein assay kit.[45] The HK activity in the supernatant was determined according to the manufacturer's instruction of the HK assay kit and expressed as nmol per min per mg protein. The absorbance was recorded at 340 nm with an ultraviolet spectrophotometer (U-3010, Hitachi, Japan).

**2.8. Intracellular ATP Determination.** Intracellular ATP levels were determined by using a CellTiter-Lumi assay kit. Briefly, cells growing in the exponential growth phase were seeded at opaque black 96-well plates with $5 \times 10^3$ cells per well (100 $\mu$L) and allowed to 24 h adherence. Afterward, the cells were incubated with LND for 24 h, followed by treatment with ACNU for 24 h. After treatment, the plates were equilibrated at room temperature for 10 min. Each well was added with 100 $\mu$L of CellTiter-Lumi Luminescent Reagent and shaken for 2 min to promote cell lysis. The plate was incubated for 10 min to stabilize the luminescence signal. The luminescence signal was recorded by a Multimode Plate Reader (PerkinElmer, Waltham, MA, USA). In the presence of ATP, the luciferase-catalyzed luciferin monooxygenation generates a luminescence signal proportional to the ATP contents.

**2.9. Determination of Cellular GSH and ROS Level.** The quantitation of cellular GSH content is based on the reaction of GSH and 5,5′-dithiobis(2-nitrobenxoic acid) to yield a yellow 2-nitro-5-thiobenzoic acid.[46] Briefly, $1 \times 10^5$ cells was seeded at each well of a six-well plate and left to adhere for 24 h. After the combination treatment of LND and ACNU, the medium containing drugs was discarded. The cells were then trypsinized and centrifuged. After removing the supernatant, the cell pellets were washed and resuspended in 0.2 mL of saline solution, followed by three-time freezing and thawing, and centrifugation to remove the cellular debris. A 0.1 mL aliquot of supernatant was taken for GSH quantitative determination according to the manufacturer's instructions. We determined the absorbance at 405 nm and determined the protein concentration using the BCA assay kit. Here, the cellular GSH content was expressed as $\mu$mol per g protein ($\mu$mol/gprot).

Intracellular ROS was monitored by staining all the cells with 2′,7′-dichloro fluorescent yellow diacetate (DCFH-DA). DCFH-DA is a fluorescence-free cell permeable dye which can be hydrolyzed by cellular esterase to generate DCFH that can be oxidized by ROS to generate a fluorescent DCF.[47] Lung cancer A549 cells were treated with indicated drugs in six-well plates. After drug treatment, each well was added with 1 mL of serum-free medium solution containing Hoechst 33342 (10 mg/mL) and DCFH-DA (10 $\mu$M) for 20 min at 37 °C. Subsequently, the cells were washed three times with fresh serum-free medium. The fluorescence intensity was detected by a fluorescence microscope (Olympus IX51, Tokyo, Japan).

**2.10. Intracellular Lactic Acid Assay.** Intracellular lactic acid was quantitated with a lactic acid assay kit. Using $NAD^+$ as an $H^+$ acceptor, lactic acid can be dehydrogenated by LDH to generate pyruvate, with the formation of NADH, in which nitrotetrazolium blue chloride is reduced to a purple color substance through the H transmission of phenazine methosulfate. The absorbance at 530 nm is linearly proportional to the lactic acid content. Briefly, cells were seeded at six-well plates ($1.5 \times 10^5$ per well, 2 mL) and allowed to incubate at 37 °C for 24 h, then treated with the combination of LND (24 h pretreatment) and ACNU (24 h treatment). Afterward, the cells were collected and lysed through repeated freezing and thawing. According to the manufacturer's protocol, a 20 $\mu$L aliquot of lysate was taken from each sample for intracellular lactic acid quantitation.

**2.11. Cell Apoptosis Analysis.** Cell apoptosis was determined using an Annexin V-FITC/PI apoptosis detection kit. Cells were seeded at six-well plates for 24 h culture and treated by LND or ACNU or LND in combination with ACNU, followed by trypsinization, centrifugation, washing with precooled PBS, and resuspension in 1 × binding buffer (100 $\mu$L). Subsequently, 5 $\mu$L of Annexin V-FITC solution and 10 $\mu$L of PI were added to the cell suspension. After incubation in the dark for 15 min, 400 $\mu$L of 1 x binding buffer was added to each well. The samples were then placed on ice, and flow cytometry analysis was performed within 1 h. Cell apoptosis were analyzed using FlowJo software (Ashland, OR, USA).

**2.12. Mitochondrial Membrane Potential Measurement.** JC-1 dye is an ideal fluorescent probe for detecting the reduction of mitochondrial membrane potential.[48] A549 cells were treated with LND for 24 h and ACNU for an additional 24 h. Afterward, the cells were collected and stained with fresh medium solution containing JC-1 and Hoechst 33342 for 20 min at 37 °C. 1 mL of staining buffer was added to the cells for


https://doi.org/10.1021/acsomega.4c00641
ACS Omega 2024, 9, 36134−36147

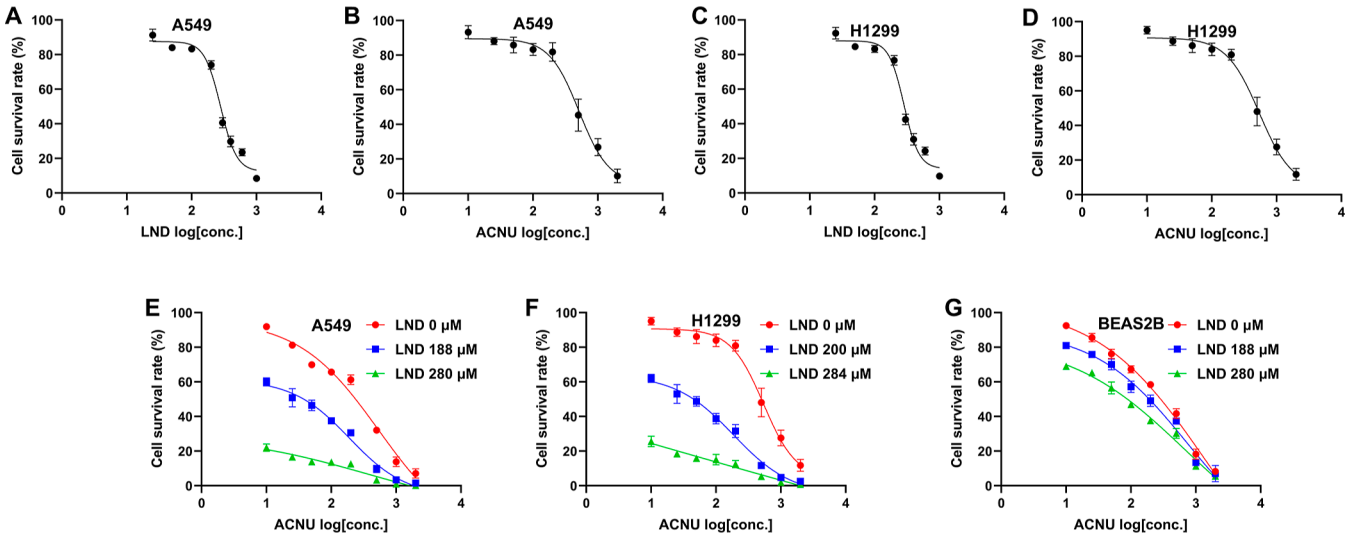


**Figure 1.** Cell survival rates of human lung cancer A549, H1299 cells, and normal lung epithelial BEAS-2B cells treated with different drugs. (A) A549 cells were treated with LND alone; (B) A549 cells were treated with ACNU alone; (C) H1299 cells were treated with LND alone; (D) H1299 cells were treated with ACNU alone; (E) A549 and (F) H1299 cells were pretreated with LND for 24 h and then treated by ACNU for 24 h; and (G) BEAS-2B cells were pretreated with LND for 24 h and then treated by ACNU for 24 h. All data are shown as mean ± SD ($n$ = 3 per group).

three washing. Finally, the mitochondrial membrane potential change was detected by using a fluorescent microscope. The JC-1 is present as a monomer with green fluorescence rather than red fluorescence when mitochondrial membrane potential is reduced.

**2.13. Western Blot Assay.** After drug treatment, the cell lysates were obtained from cells treated with different drugs using RIPA lysis buffer supplemented with 1 mM PMSF. The protein concentration in the supernatant was quantified by the BCA protein assay kit.[45] After mixing with loading buffer, the protein sample was denatured at 95 °C for 5 min. Approximately 60 $\mu$g of protein per sample was loaded in 12% SDS-PAGE gel, transferred to poly(vinylidene difluoride) membrane (Millipore Inc., Billerica, MA, USA), blocked overnight, incubated with primary antibody at 1:1000 (rabbit monoclonal anti-MGMT/anti-MMP2 antibodies) or 1:10,000 (mouse monoclonal anti-$\beta$-actin antibody) at 4 °C for 12 h, and incubated with preadsorbed goat antimouse or antirabbit IgG second antibody (IRDye 800CW) at room temperature for 1 h. The bands were captured by an Odyssey infrared imaging system (LI-COR Biosciences, Lincoln, NE, USA). The $\beta$-actin was used as a reference protein.

**2.14. Determination of DNA ICLs.** The DNA ICLs in human lung cancer A549 cells after drug combination treatment were determined by single-cell gel electrophoresis.[49] A549 cells were seeded in T25 culture flasks and cultured until the cell density reached approximately 90%, followed by treatment with LND (24 h pretreatment) and ACNU (24 h treatment), respectively. To distinguish cross-linked and un-cross-linked DNA, 100 $\mu$L of 0.3% $H_2O_2$ solution was added to cells for 20 min treatment on ice to induce DNA strand breaks. The reaction was quenched by adding 1% (v/v) DMSO. Subsequent steps were performed according to the DNA damage detection kit. Cells were embedded in agarose, electrophoresed under alkaline conditions, and stained by PI. Images were captured by fluorescence microscopy, where the single cell revealed a comet-like form. Here, cross-linked DNA migrates slowly and presents as the round comet "head", whereas the broken DNA yields the "tail". The analysis was performed using the Comet Assay Software Project. The DNA ICL rate was calculated as the decrease in percentage of olive tail moment (OTM) in cells treated with indicated drugs and $H_2O_2$ relative to cells treated with only $H_2O_2$.[49,50] The percent decrease representing the level of ICLs was calculated as follows:

$$\left(1 - \frac{\mathrm{OTM(drug + H_2O_2) - OTM(drug) - OTM(control)}}{\mathrm{OTM(H_2O_2) - OTM(control)}}\right) \times 100$$

where OTM (control), OTM ($H_2O_2$), OTM (drug), and OTM (drug + $H_2O_2$) indicate the OTM of cells treated with neither drug nor $H_2O_2$, with only $H_2O_2$, with only drug, and with both drug and $H_2O_2$, respectively.

**2.15. Statistical Analysis.** Graphpad Prism 8.0 software was used for statistical analysis. Unless otherwise stated, all results were calculated from at least three independent experiments and expressed as the mean ± the standard deviation. Two-tailed standard Student's $t$-test was performed to determine the significance between two groups (paired one-tail $t$-test for Western blot analysis). *$p < 0.05$, **$p < 0.01$, and ***$p < 0.001$ indicate significant statistical difference between different groups.

## 3. RESULTS AND DISCUSSION

**3.1. LND Enhanced the Sensitivity of Human Lung Cancer Cell Lines to ACNU.** As a single agent, LND is shown to have limited anticancer activity; however, it exhibits unique potential to modulate the chemotherapeutic effects of conventional drugs: (1) tumor selectivity; (2) low toxicity to normal cells; and (3) multiple biochemical mechanisms, including inhibiting glycolysis, mitochondrial respiration, lactate efflux, and pyruvate uptake.[35−37] Here, we compared the effects of LND and ACNU, either alone or in combination, on the survival of human lung cancer A549 cells using an MTT method.

As shown in Figure 1A,B, LND or ACNU alone decreased the cell survival rate in a dose-dependent manner in A549 cells.



https://doi.org/10.1021/acsomega.4c00641
ACS Omega 2024, 9, 36134−36147

Table 1. Combination Index ($Q$)[a] of LND and ACNU in Human Lung Cancer A549, H1299 Cells, and Normal Lung Epithelial BEAS-2B Cells

| A549 | | | H1299 | | | BEAS-2B | | |
|---|---|---|---|---|---|---|---|---|
| LND ($\mu$M) | ACNU ($\mu$M) | $Q^a$ | LND ($\mu$M) | ACNU ($\mu$M) | $Q^a$ | LND ($\mu$M) | ACNU ($\mu$M) | $Q^a$ |
| 188 | 10 | 1.31 | 200 | 10 | 1.29 | 188 | 10 | 0.97 |
| 188 | 25 | 1.25 | 200 | 25 | 1.24 | 188 | 25 | 0.95 |
| 188 | 50 | 1.13 | 200 | 50 | 1.17 | 188 | 50 | 0.89 |
| 188 | 100 | 1.24 | 200 | 100 | 1.28 | 188 | 100 | 1.03 |
| 188 | 200 | 1.28 | 200 | 200 | 1.23 | 188 | 200 | 1.03 |
| 188 | 500 | 1.21 | 200 | 500 | 1.22 | 188 | 500 | 0.98 |
| 188 | 1000 | 1.07 | 200 | 1000 | 1.14 | 188 | 1000 | 1.03 |
| 188 | 2000 | 1.04 | 200 | 2000 | 1.13 | 188 | 2000 | 1.00 |
| 280 | 10 | 1.46 | 284 | 10 | 1.48 | 280 | 10 | 1.12 |
| 280 | 25 | 1.42 | 284 | 25 | 1.43 | 280 | 25 | 1.05 |
| 280 | 50 | 1.32 | 284 | 50 | 1.33 | 280 | 50 | 1.08 |
| 280 | 100 | 1.29 | 284 | 100 | 1.27 | 280 | 100 | 1.12 |
| 280 | 200 | 1.26 | 284 | 200 | 1.29 | 280 | 200 | 1.15 |
| 280 | 500 | 1.16 | 284 | 500 | 1.15 | 280 | 500 | 1.03 |
| 280 | 1000 | 1.06 | 284 | 1000 | 1.09 | 280 | 1000 | 1.03 |
| 280 | 2000 | 1.03 | 284 | 2000 | 1.06 | 280 | 2000 | 1.01 |

[a]$Q$ is the combination index derived from the formula: $Q = E_{(A+B)}/(E_A + E_B - E_A \times E_B)$, in which $E_{(A+B)}$ indicates the cell killing rate of combination treatment; $E_A$ and $E_B$ indicate the cell killing rates of drug A (LND) and B (ACNU), respectively. $Q > 1.15$, synergism; $Q < 0.85$, antagonism; $0.85 \leq Q \leq 1.15$, additive.

The $IC_{25}$ and $IC_{50}$ values were 188 and 280 $\mu$M for LND, and 225 and 512 $\mu$M for ACNU, respectively. When LND (24 h pretreatment) was used in combination with ACNU (24 treatment), we found the survival rate of A549 cells significantly decreased compared to ACNU alone (Figure 1E). As seen in Table 1, we calculated the combination index using Jin's formula.[44] It is very clear that LND in combination with ACNU exhibited a synergistic killing effect in A549 cells, the Q values ranged from 1.03−1.46 ($Q > 1.15$: synergistic effect, $Q < 0.85$: antagonistic effect, and $0.85 \leq Q \leq 1.15$: additive effect). To further validate the generalizability of the findings, we also explored the synergistic effect of the combination in H1299 cells. As shown in Figure 1F, LND in combination with ACNU also produced a synergistic killing effect in H1299 cells (Table 1). In addition, to verify the combination effect of LND and ACNU in normal cells, we evaluated the combination index Q in normal lung epithelial BEAS-2B cell line. As expected, we did not observe a remarkable increase in ACNU-induced cytotoxicity after LND pretreatment (Figure 1G). The combination index also confirmed this result (Table 1). However, it should be noted that LND and ACNU had an additive effect in BEAS-2B cell line; possible off-target effects need further exploration. From the cytotoxicity assay, LND showed a promising chemosensitization effect for ACNU in lung cancer cells rather than normal lung epithelial cells. These results also indicate the beneficial role of LND as a chemosensitizer when in combination with conventional chemotherapeutic agents to some extent.

**3.2. Combined Effects of LND and ACNU on Cell Apoptosis, Colony Formation, Migration, and Invasion of Human Lung Cancer A549 Cells.** After the cytotoxicity assay, we also determined the apoptosis-inducing effects using the Annexin V-FITC/PI apoptosis assay kit. As shown in Figure 2, compared to LND or ACNU alone, LND in combination with ACNU significantly increased the apoptosis rate in the human lung cancer A549 cell line.

To investigate whether LND could enhance the inhibitory effect of ACNU on the growth of A549 cells, we performed the colony formation assay. Initially, the $IC_{25}$ and $IC_{50}$ values of ACNU or LND were measured under colony formation assay (Figure 3A and 3B). LND or ACNU reduced the cell proliferation in a dose-dependent manner, and the $IC_{25}$ and $IC_{50}$ values were 87 and 232 $\mu$M for LND, and 19 and 55 $\mu$M for ACNU, respectively. As shown in Figure 3C,D, the combination of LND and ACNU significantly reduced the proliferation of A549 cells when compared with ACNU or LND alone. For example, almost no colonies were generated in the group treated with the combination of 232 $\mu$M LND and 55 $\mu$M ACNU. This result indicates that LND pretreatment can enhance the growth inhibitory effect of ACNU against human lung cancer cells.

The cell migration and repair ability after drug treatment were also determined by the migration assay. As depicted in Figure 4A, the wound was almost completely healed at 48 h in the control group. In combined treatment groups, the migration rates were remarkably lower than those of single drug groups (Figure 4B). It should be noted that 188 $\mu$M LND combined with 225 or 512 $\mu$M ACNU, and 280 $\mu$M LND combined with 225 or 512 $\mu$M ACNU significantly inhibited the migration of A549 cells at 48 h compared with groups without LND pretreatment. The results indicate that LND and ACNU have a synergy in inhibiting the migration of A549 cell and the wound repair.

The metastatic ability after drug treatment was further investigated by a transwell assay. By comparing the number of invaded cells, we found LND remarkably strengthened the inhibition of ACNU on the invasion ability of A549 cells than ACNU alone (Figure 5A,B). For example, the invasion rates of groups exposed to 280 $\mu$M LND combined with 225 or 512 $\mu$M ACNU decreased by 48 and 37% when compared with ACNU alone, respectively. The invasion assay indicated that LND in combination with ACNU produced a significant suppression of the invasion of the human lung cancer A549 cell


https://doi.org/10.1021/acsomega.4c00641
ACS Omega 2024, 9, 36134−36147

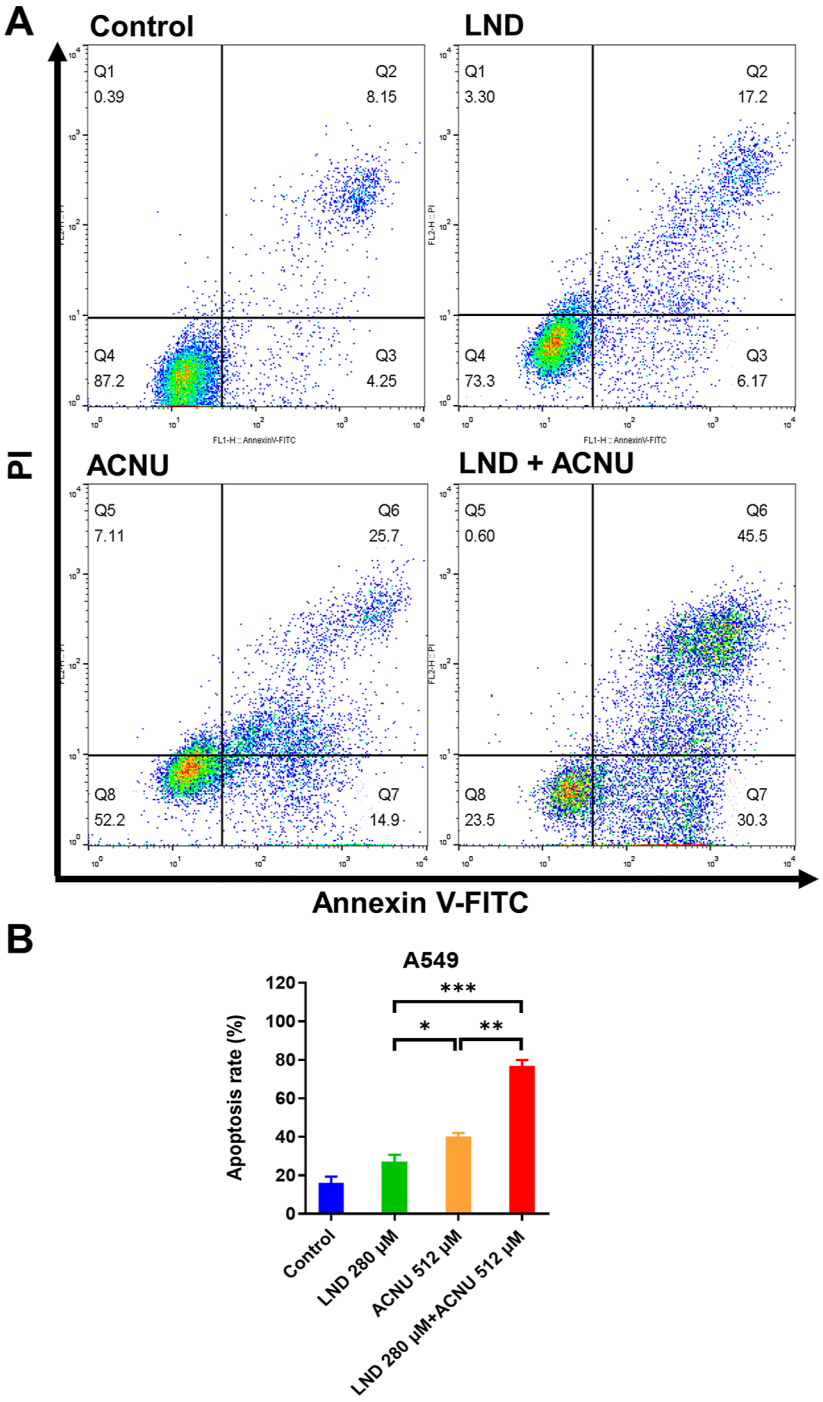


**Figure 2.** Apoptosis in A549 cells after the combination treatment of LND (24 h pretreatment) and ACNU (24 h treatment). (A) Distribution of apoptotic cells using flow cytometry and (B) apoptosis rates in different groups. All data are shown as mean ± SD ($n$ = 3). *$p$ < 0.05, **$p$ < 0.01, and **$p$ < 0.001 indicate the statistical difference between different groups.

line. Thus, the combination strategy may have the potential to inhibit clinical tumor metastasis.

In addition, migration- and invasion-related protein matrix metalloproteinase-2 (MMP2) was also checked by Western blotting. LND is known to disrupt cellular energy metabolism, leading to a reduced ATP level and increased oxidative stress. ACNU, a cytotoxic alkylating agent, induces DNA damage and can affect the expression of genes involved in cell survival and apoptosis. These changes may influence the expression and activity of various proteins involved in cell migration and invasion, including MMPs. As seen in Figure 5C,D, it is obvious that MMP2 expression was significantly decreased in cells treated with ACNU alone or LND in combination with ACNU when compared to the control group. It should be clarified that the apoptosis-inducing effects did not completely follow the same trends as the invasion results, indicating that invasion inhibition may be independent of apoptosis induction. Especially, we noticed that LND alone did not show any inhibition on MMP2 expression, and the combination of LND and ACNU had no obvious difference with ACNU alone on MMP2 expression, implying the lack of additive or synergistic inhibition of MMP2 by the combination of LND and ACNU


https://doi.org/10.1021/acsomega.4c00641
ACS Omega 2024, 9, 36134−36147

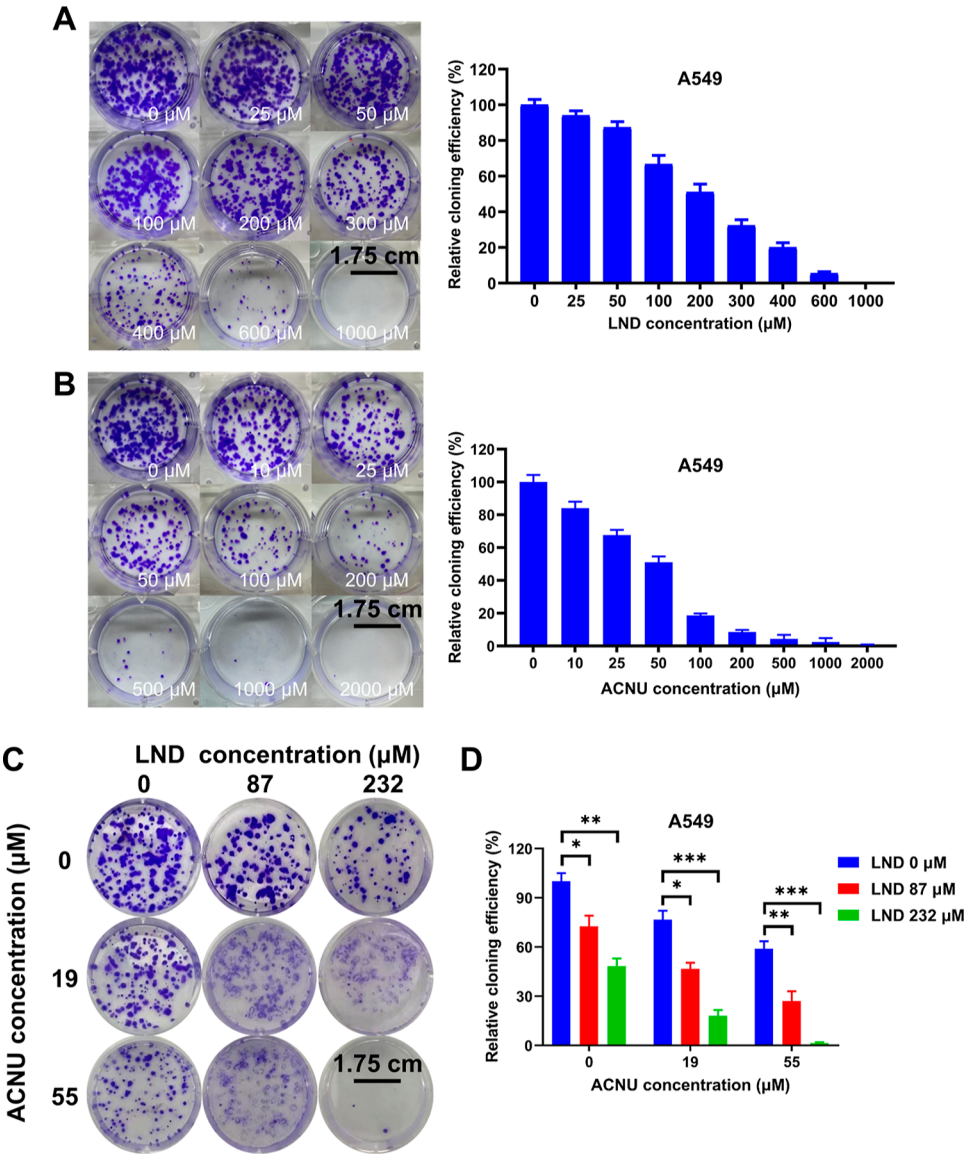


**Figure 3.** Colony formation ability of A549 cell line after exposure to different formulations. Cells were treated with increasing concentrations of (A) LND or (B) ACNU for 24 h; (C,D) colony images and efficiency of cells pretreated with LND for 24 h, followed by exposure to ACNU for 24 h, respectively. All data are shown as mean ± SD ($n$ = 3). *$p$ < 0.05, **$p$ < 0.01, and **$p$ < 0.001 vs ACNU alone treated groups.

(Figure 5D), which should be due to the existence of other migration/invasion-related proteins (e.g., MMP9) affected by LND.

**3.3. LND in Combination with ACNU Induced De-energization through Inhibiting Glycolysis and Mitochondrial Dysfunction.** To explore the mechanism of enhanced ACNU sensitivity mediated by LND in the human lung cancer A549 cell line, we determined the influence of the combination of LND and ACNU on glycolysis and mitochondrial membrane potential. In previous studies, LND was reported to inhibit HK activity and disrupt mitochondria, thereby cutoff the energy supply for tumor cell proliferation.[51,52] First, we measured the HK activity in the A549 cells after drug treatment. It was found that ACNU almost had no influence on HK activity, while LND exhibited a dose-dependent decrease of HK activity (Figure 6A). The combination of LND and ACNU further decreased the HK activity; however, even 280 $\mu$M LND in combination with 512 $\mu$M ACNU only produced a moderate decrease (less than 40%) compared to the control group (Figure 6A). In this case, the decreasing degree of HK activity should be not sufficient to markedly reduce intracellular ATP levels.

Mitochondrion is also a potential target of LND that can induce permeability transition pore opening in mitochondrial membrane and inhibit complex II in respiratory chain, leading to the reduction of transmembrane potential.[29,37,53,54] As depicted in Figure 6B, LND alone produced an increasing green fluorescence, while a slight effect was found in ACNU-treated groups. When LND was combined with ACNU, more green fluorescence was generated, accompanied by a gradual fading of red fluorescence. This result indicates that the combination of LND and ACNU could produce a more significant decrease in mitochondrial membrane potential.

The above results showed that both glycolytic inhibition and mitochondrial dysfunction are generated under the combination of LDN and ACNU. This should result in the downregulation of intracellular energy levels. As seen in Figure 6C, compared with LND alone, LND combined with ACNU


https://doi.org/10.1021/acsomega.4c00641
ACS Omega 2024, 9, 36134−36147

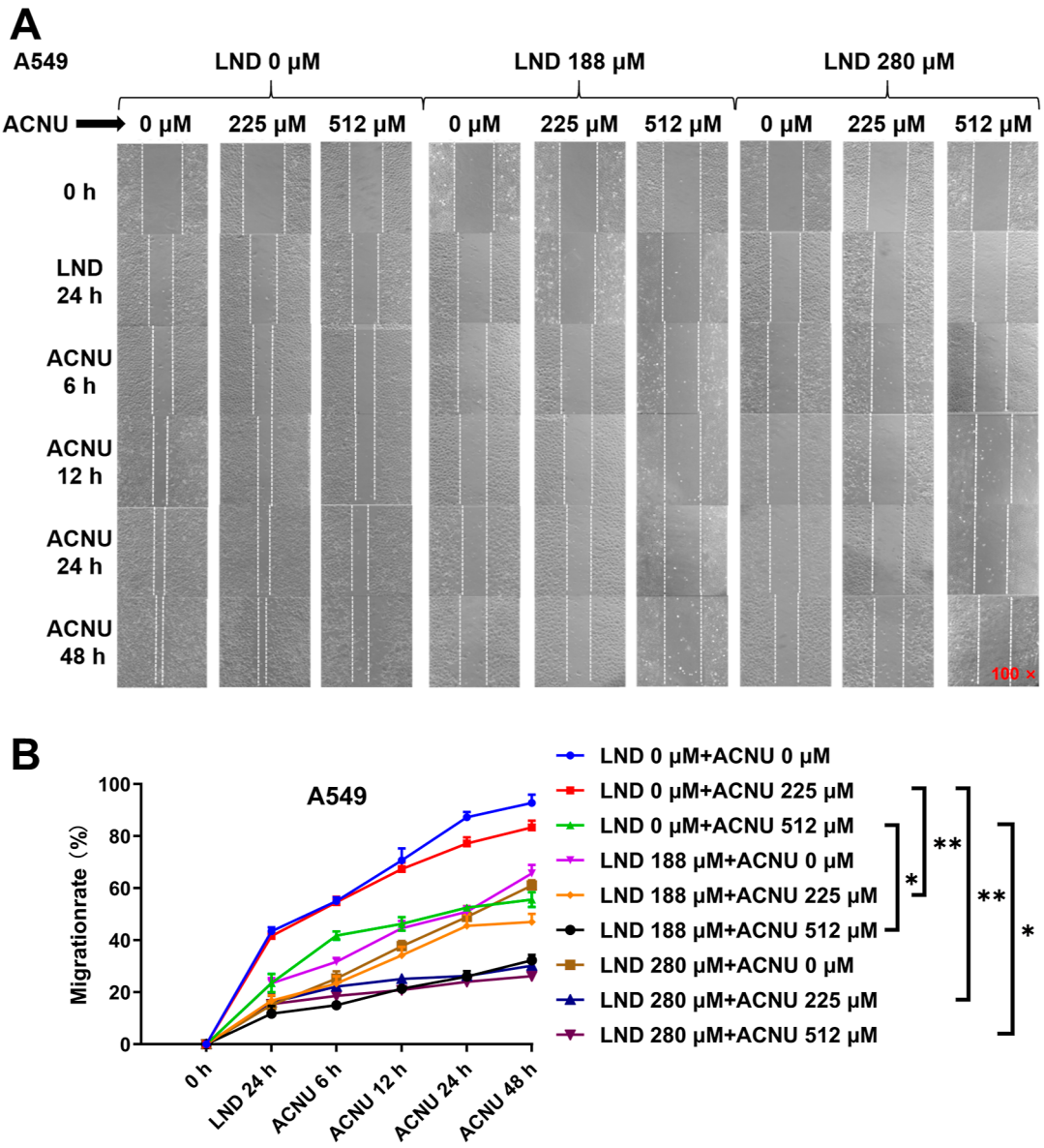


**Figure 4.** Cell migration of A549 cells cotreated with LND (24 h pretreatment) and ACNU (0−48 h). (A) Wound healing status at various time points; (B) quantitative analysis of the migration rates in different groups. All data are shown as mean ± SD ($n$ = 3). *$p$ < 0.05, **$p$ < 0.01 vs ACNU alone treated groups.

remarkably reduced intracellular ATP levels. Because the increased drug efflux is closely associated with the intracellular ATP level,[20,23,26,55] the significant de-energization by LND in combination with ACNU should overcome the ATP-mediated MDR and DNA damage repair, increasing the tumor killing effect.

**3.4. Influence of Combination Treatment on Redox State of Human Lung Cancer A549 Cells.** The mitochondrial dysfunction induced by LND or its combination with ACNU may result in the ROS formation because complex II is a source of ROS when the respiratory chain is inhibited.[56] On the other hand, the partial glycolytic inhibition by LND should downregulate the pentose phosphate pathway which is a major source of cellular reduced substances.[29,37] Thus, we explored the effect of LND in combination with ACNU on the cellular redox state of A549 cells by determining the GSH and ROS levels.

As shown in Figure 7A, LND or ACNU alone produced a dose-dependent decrease in the cellular GSH contents. ACNU-induced GSH decrease should be derived from the reaction of GSH with parent drug or its decomposed intermediates.[21,22,57] The combined treatment further decreased the cellular GSH contents compared to those of ACNU or LND alone. For instance, after exposure to 188 $\mu$M or 288 LND combined with 512 $\mu$M ACNU, approximately 38 and 44% GSH reduction was observed with respect to the control group.

The ROS levels in A549 cells were determined using DCFH-DA fluorometry (Figure 7B,C). The green fluorescence indicates the ROS existence. Similar to the change of cellular GSH contents, the combination treatment of LND and ACNU induced significantly higher ROS levels than single drug group. On the contrary, the addition of NAC neutralized the induction of ROS (Figure 7B,C), indicating that the redox homeostasis disruption is indeed caused by LND.



https://doi.org/10.1021/acsomega.4c00641
ACS Omega 2024, 9, 36134−36147

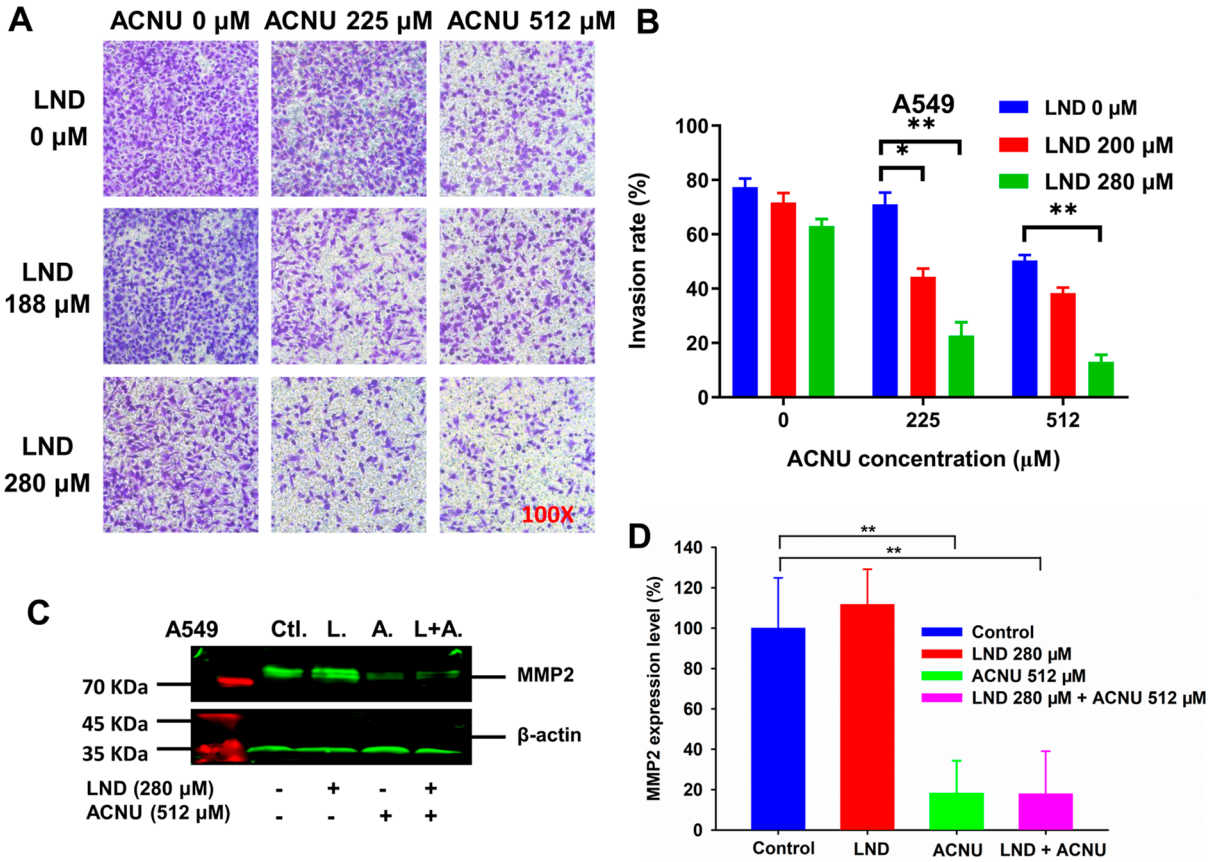


**Figure 5.** Invasion ability and MMP2 expression level of A549 cells after the combination treatment with LND (24 h pretreatment) and ACNU (24 h treatment). (A) Images of invaded cells; (B) invasion rates of cells treated by different drugs; (C) Western blotting bands; and (D) quantitative analysis of MMP2 protein expression levels. All data are shown as mean ± SD ($n = 3$; $n = 4$ for Western blotting). *$p < 0.05$ and **$p < 0.01$ indicate the statistical difference between any two groups.

As we know, GSH is involved in drug detoxification through chemical conjugation, leading to the development of chemoresistance.[21] Meanwhile, ROS can induce cell apoptosis via causing DNA oxidative damage.[58] Thus, ROS generation and GSH quenching by the combination of LND and ACNU should promote the tumor killing effect.

**3.5. LND Significantly Induced Intracellular Acidification and Downregulated MGMT Expression in A549 Cells.** Previous study[59] indicates that LND can inhibit monocarboxylate transporter and mitochondrial pyruvate carrier, respectively, which may lead to the accumulation of lactate in cytoplasm thus intracellular acidification of tumors. Ben-Yoseph et al. demonstrated that LND inhibited lactate efflux and induced intracellular acidification in rat 9L tumor cells in vitro and in vivo.[35] Notably, LND did not exert any influence on the intracellular pH and energy metabolism of the brain and skeletal muscle. Nath and co-workers showed that in human DB-1 melanoma mice xenografts, LND-caused acidification could stabilize the active intermediates of N-mustard drugs and inhibit GST that is critical for GSH formation.[36,38] Moreover, the authors suggested that intracellular acidification may inhibit MGMT expression and thus DNA damage repair.[36,37] Nevertheless, to the best of our knowledge, there is no clear experimental evidence that intracellular acidification inhibits MGMT expression in human lung cancer cells.

Here, we determined the lactate levels after drug treatment and MGMT expression levels. As shown in Figure 8A, ACNU alone had no any influence on the intracellular lactate content of A549 cells. On the contrary, LND alone induced a dose-dependent increase in the intracellular lactate content. Notably, the combination of LND and ACNU further enhanced the levels of intracellular lactate.

As a DNA repair protein, MGMT can transfer the alkyl groups at guanine $O^6$ position to its active site Cys145 residue, thus conferring resistance to the anticancer alkylating agent like ACNU, BCNU, and TMZ.[13] Therefore, effective downregulation of MGMT expression is crucial for improving the chemotherapeutic effects of these agents.[60,61] We determined the MGMT expressing levels in A549 cells after drug treatment using Western blot. As seen in Figure 8B,C, ACNU alone had no influence on the MGMT expression. On the contrary, LND alone significantly downregulated the expression of MGMT (less than 10% control). The combination of LND and ACNU almost completely inhibited the MGMT expression. The purpose of setting up the combination treatment group of LND and ACNU is to verify the effectiveness of MGMT downregulation and ensure the blockade of MGMT-mediated DNA repair in the combination strategy.

The above results provided sufficient evidence that LND could inhibit MGMT expression by intracellular acidification and thus may weaken the repair of DNA cross-linking precursors in tumor cells and lead to enhanced antitumor activity of ACNU.

**3.6. Effect of LND on the Formation of DNA ICLs Induced by ACNU.** The antitumor activity of ACNU and related alkylating agents is mainly associated with the


https://doi.org/10.1021/acsomega.4c00641
ACS Omega 2024, 9, 36134−36147

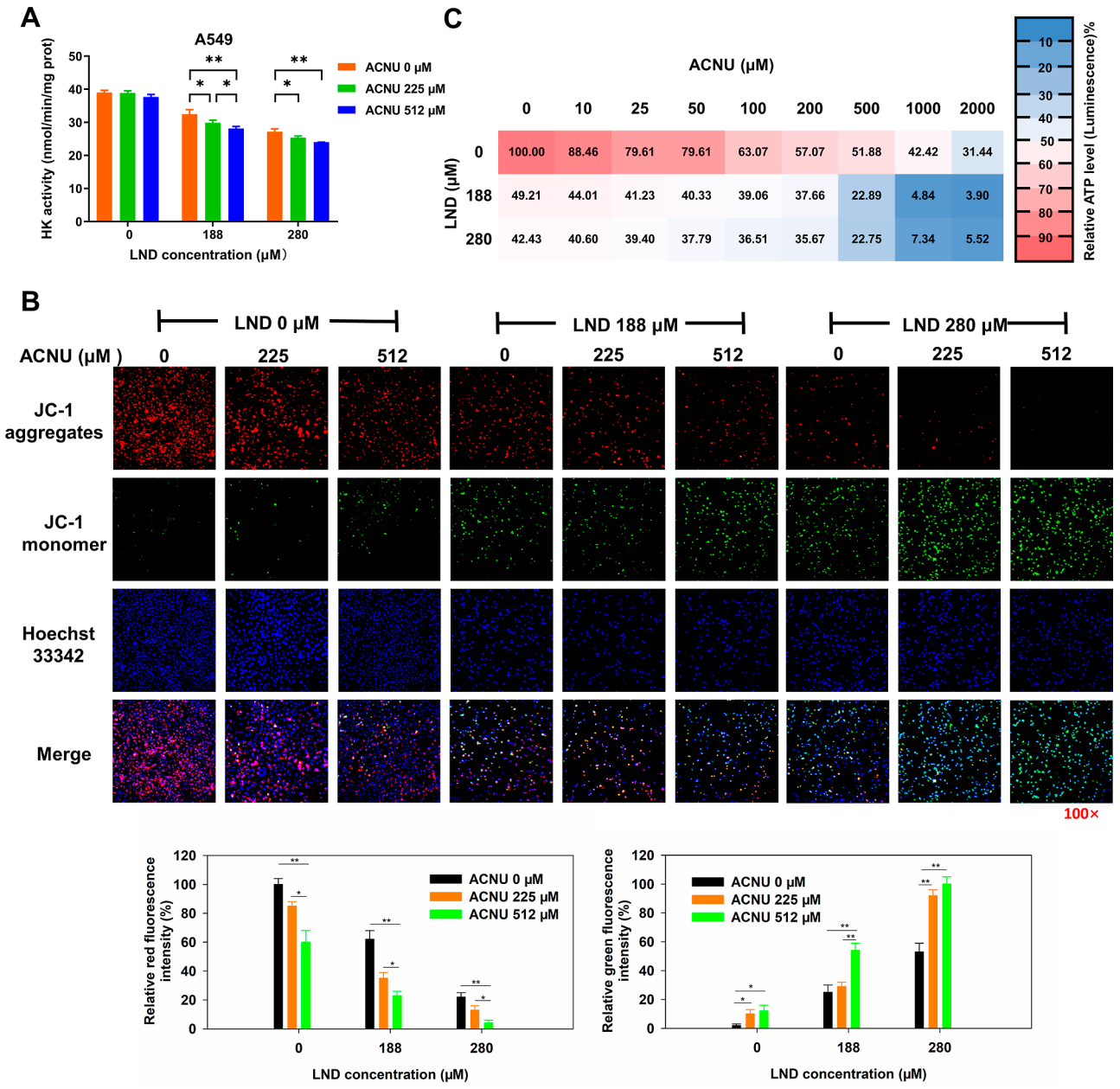


**Figure 6.** Influence of LND (24 h pretreatment) in combination with ACNU (24 h treatment) on (A) HK activity, (B) mitochondrial membrane potential by JC-1 staining, and (C) intracellular ATP levels. All data are shown as mean ± SD ($n$ = 3). *$p$ < 0.05 and **$p$ < 0.01 indicate the statistical difference between any two groups.

formation of DNA ICLs that can induce apoptosis via inhibiting DNA replication and transcription.[11,12,62] In this work, based on the results of LND-induced energy blockade, MGMT and GSH downregulation reduction, it is speculated that LND should enhance the amount of DNA ICLs induced by ACNU. Thus, we determined the levels of DNA ICLs using alkaline comet assay[49,50] in A549 cells after drug treatment. After exposure to indicated drugs, $H_2O_2$ was added to induce DNA strand breaks so that the cross-linked DNA can be distinguished from uncross-linked DNA. In comet assay, cross-linking can prevent the mobility of DNA and decrease DNA content in comet tail, thus shortening the comet tail length. The levels of DNA ICLs in A549 cells were calculated by the decreasing degree of DNA migration relative to the $H_2O_2$ alone treated group. The comet electrophoresis showed that LND alone almost produced no DNA ICLs (Figure 9). As expected, as a DNA cross-linking agent, ACNU alone yielded an obvious decrease in comet tail moment (~60%), suggesting the generation of DNA ICLs. When cells were pretreated with LND, we found a significant increase of the decreasing degree (~75%) in tail moment, indicating an increasing level of ACNU-induced DNA ICLs in A549 cells. The comet assay suggests that LND can further enhance the levels of DNA ICLs induced by ACNU.

## 4. CONCLUSIONS

In this study, we demonstrated that energy metabolism inhibitor LND can increase the sensitivity of human lung cancer A549 cell line to anticancer alkylating agent ACNU. The underlying mechanisms of LND in modulating ACNU sensitivity include: glycolytic inhibition and mitochondrial


https://doi.org/10.1021/acsomega.4c00641
ACS Omega 2024, 9, 36134−36147

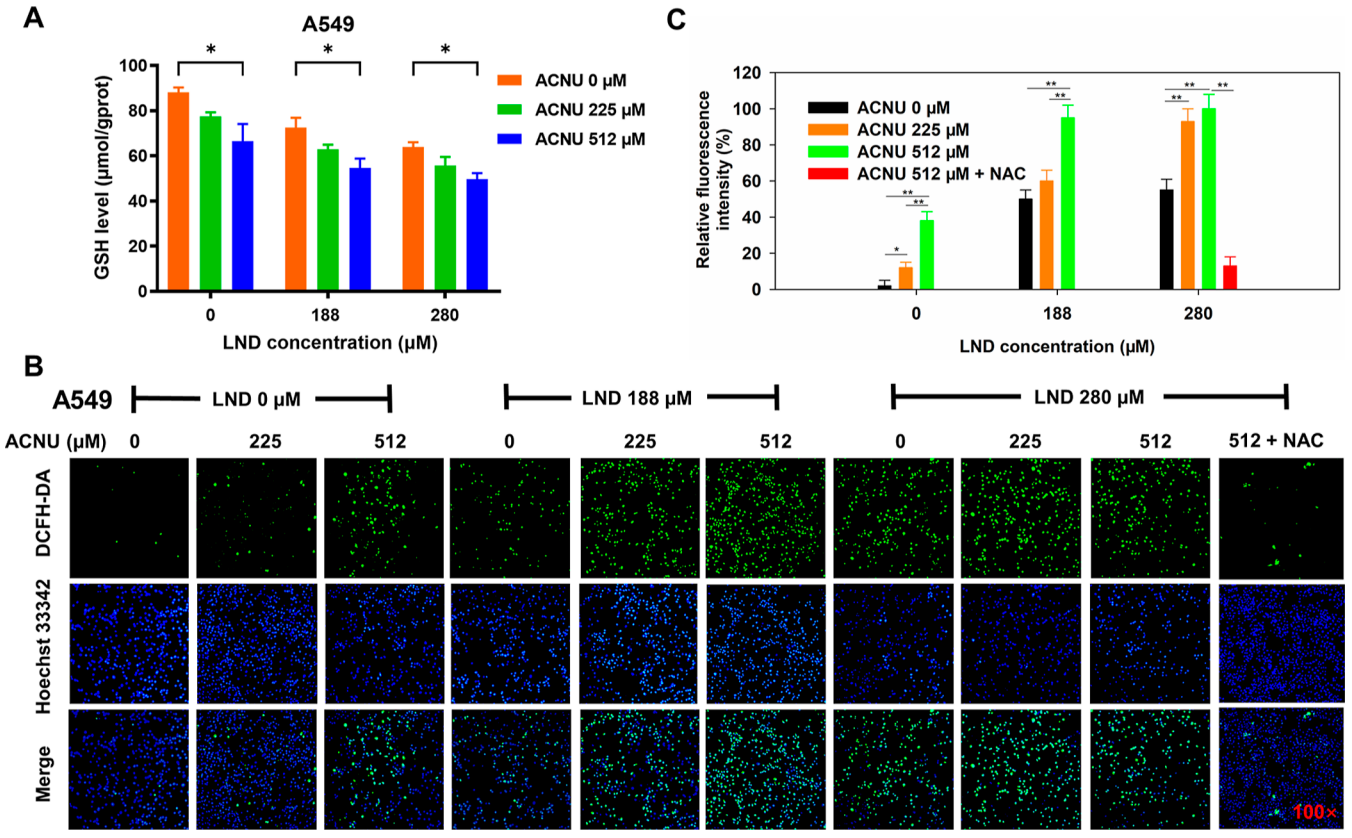


**Figure 7.** Influence of LND (24 h pretreatment) in combination with ACNU (24 h treatment) on (A) GSH contents and (B) ROS levels of A549 cells. The addition of NAC (1 mM) was used as the control group. (C) Quantitation of fluorescence intensity presenting the ROS levels in A549 cells. All data are shown as mean ± SD ($n$ = 3). *$p$ < 0.05 vs LND alone.

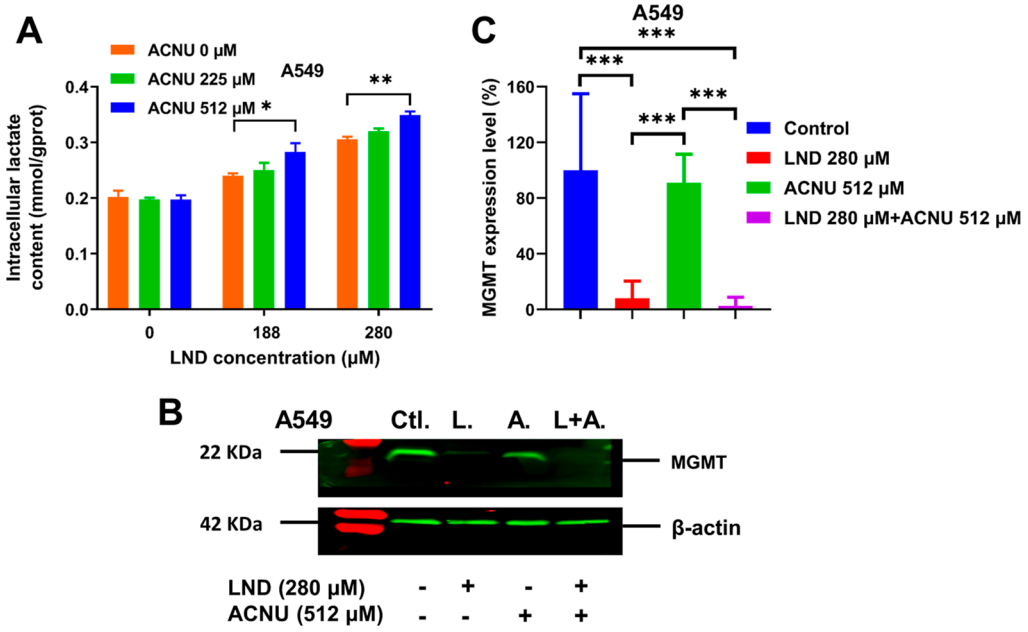


**Figure 8.** Influence of different drug treatments on (A) intracellular lactate levels, (B) MGMT expression of A549 cells, and (C) quantitative analysis of at least three independent experiments. All data are shown as mean ± SD ($n$ = 3). *$p$ < 0.05, *$p$ < 0.01, and *$p$ < 0.001 indicate the statistical difference between two groups (paired one-tail $t$-test for Western blotting analysis).

dysfunction, GSH decrease and ROS generation, and MGMT downregulation via intracellular acidification. As a result, the formation of DNA ICLs induced by ACNU was significantly enhanced by LND pretreatment. Interestingly, lung cancer cell metastasis may also be inhibited by the combination of LND and ACNU in a clinical setting. In terms of the analysis results of multiple biochemical indexes, drug resistance is mainly cut off at three aspects, namely, DNA damage repair, drug



https://doi.org/10.1021/acsomega.4c00641
ACS Omega 2024, 9, 36134−36147

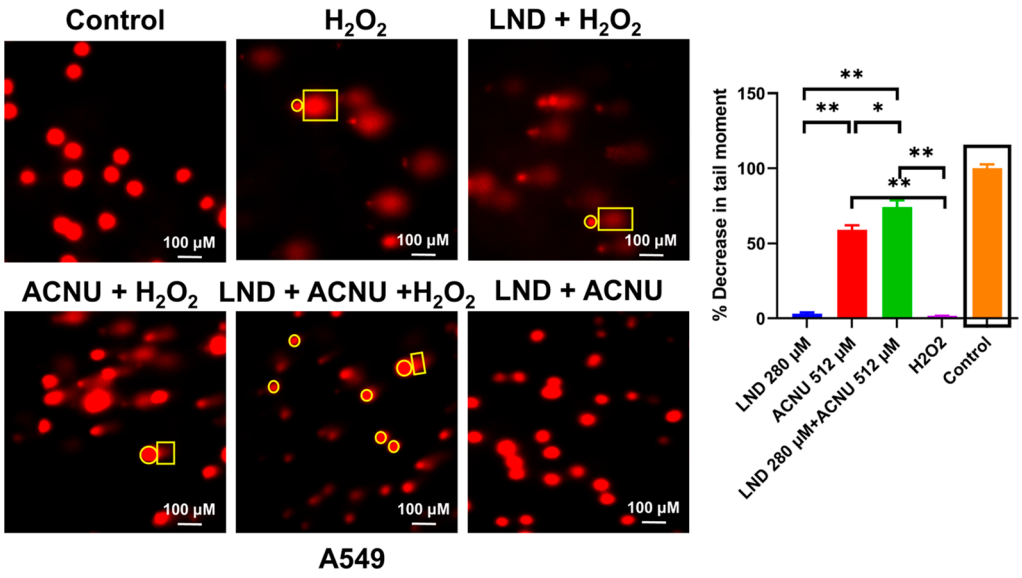


**Figure 9.** Quantitative analysis of ACNU-induced DNA ICLs in A549 cells with or without LND pretreatment using alkaline comet assay (head: circle and tail: rectangle). LND alone treated group was used as the negative control group. All data are shown as mean ± SD ($n$ = 3). *$p$ < 0.05 and *$p$ < 0.01 indicate the statistical difference between two groups.

inactivation, and drug efflux. In other words, LND increases the antitumor effect of ACNU via energy inhibition, disrupting redox homeostasis and downregulating MGMT expression in the human lung cancer cell line. Notably, whether the relatively high drug concentrations in vitro will result in the effectiveness, in vivo or clinical setting remains to be solved. Moreover, the combination strategy of LND and ACNU should be validated on multiple tumor cells. This combined treatment strategy using LND as a chemosensitizer warrants further investigation in both preclinical and clinical trials. These findings suggest that incorporating LND into ACNU-based therapies could potentially improve treatment outcomes for lung cancer patients.

## ■ ASSOCIATED CONTENT

### Supporting Information

The Supporting Information is available free of charge at https://pubs.acs.org/doi/10.1021/acsomega.4c00641.

Original Western blotting with four repeated results for MMP2 expression and five repeated results for MGMT expression (DOCX)

## ■ AUTHOR INFORMATION


### Corresponding Authors

**Xin Wang** − *Department of Clinical Trials Center, National Cancer Center/National Clinical Research Center for Cancer/Cancer Hospital, Chinese Academy of Medical Sciences and Peking Union Medical College, Beijing 100029, P. R. China*; Email: xiaowuxian2006@126.com

**Peng Wang** − *Department of Neurosurgery, the First Medical Center of Chinese PLA General Hospital, Beijing 100853, P. R. China*; Email: wangpeng301@foxmail.com

**Guohui Sun** − *Beijing Key Laboratory of Environment & Viral Oncology, College of Chemistry and Life Science, Beijing University of Technology, Beijing 100124, P. R. China*; orcid.org/0000-0003-2259-5431; Email: sunguohui@bjut.edu.cn

### Authors

**Tengjiao Fan** − *Department of Medical Technology, Beijing Pharmaceutical University of Staff and Workers, Beijing 100079, P. R. China; Beijing Key Laboratory of Environment & Viral Oncology, College of Chemistry and Life Science, Beijing University of Technology, Beijing 100124, P. R. China*

**Lin Shen** − *Department of Dermatology, the First Medical Center of PLA General Hospital, Beijing 100853, P. R. China*

**Yaxin Huang** − *Beijing Key Laboratory of Environment & Viral Oncology, College of Chemistry and Life Science, Beijing University of Technology, Beijing 100124, P. R. China*

**Lijiao Zhao** − *Beijing Key Laboratory of Environment & Viral Oncology, College of Chemistry and Life Science, Beijing University of Technology, Beijing 100124, P. R. China*; orcid.org/0000-0002-4876-323X

**Rugang Zhong** − *Beijing Key Laboratory of Environment & Viral Oncology, College of Chemistry and Life Science, Beijing University of Technology, Beijing 100124, P. R. China*

Complete contact information is available at: https://pubs.acs.org/10.1021/acsomega.4c00641

### Author Contributions

#T.F. and L.S. contributed equally to this work.


### Notes

The authors declare no competing financial interest.

## ■ ACKNOWLEDGMENTS

This work was supported by the Beijing Natural Science Foundation (nos. 7242193 and 7222016), the National Natural Science Foundation of China (no. 82003599), the Project of Cultivation for Young Top-Motch Talents of Beijing Municipal Institutions (no. BPHR202203016), and the Science and Technology General Project of Beijing Municipal Education Commission (no. KM202110005005).

## ■ REFERENCES

(1) Sung, H.; Ferlay, J.; Siegel, R. L.; Laversanne, M.; Soerjomataram, I.; Jemal, A.; Bray, F. Global cancer statistics 2020:

GLOBOCAN estimates of incidence and mortality worldwide for 36 cancers in 185 countries. *Ca-Cancer J. Clin.* **2021**, *71* (3), 209−249.
(2) Wu, Q.; Qian, W.; Sun, X.; Jiang, S. Small-molecule inhibitors, immune checkpoint inhibitors, and more: FDA-approved novel therapeutic drugs for solid tumors from 1991 to 2021. *J. Hematol. Oncol.* **2022**, *15* (1), 143.
(3) Hanahan, D. Hallmarks of Cancer: New Dimensions. *Cancer Discov.* **2022**, *12* (1), 31−46.
(4) Sun, G. H.; Fan, T. J.; Zhao, L. J.; Zhou, Y.; Zhong, R. G. The potential of combi-molecules with DNA-damaging function as anticancer agents. *Future Med. Chem.* **2017**, *9* (4), 403−435.
(5) Guohui, S.; Lijao, Z.; Rugang, Z. The induction and repair of DNA interstrand crosslinks and implications in cancer chemotherapy. *Anti-Cancer Agents Med. Chem.* **2016**, *16* (2), 221−246.
(6) Nikolova, T.; Roos, W. P.; Kramer, O. H.; Strik, H. M.; Kaina, B. Chloroethylating nitrosoureas in cancer therapy: DNA damage, repair and cell death signaling. *Biochim. Biophys. Acta Rev. Cancer* **2017**, *1868* (1), 29−39.
(7) Sun, G. H.; Zhao, L. J.; Fan, T. J.; Li, S. S.; Zhong, R. G. Investigations on the effect of O6-benzylguanine on the formation of dG-dC interstrand cross-links induced by chloroethylnitrosoureas in human glioma cells using stable isotope dilution high-performance liquid chromatography electrospray ionization tandem mass spectrometry. *Chem. Res. Toxicol.* **2014**, *27* (7), 1253−1262.
(8) Erickson, L. C.; Laurent, G.; Sharkey, N. A.; Kohn, K. W. DNA cross-linking and monoadduct repair in nitrosourea-treated human tumour cells. *Nature* **1980**, *288* (5792), 727−729.
(9) Kaina, B.; Margison, G. P.; Christmann, M. Targeting O6-methylguanine-DNA methyltransferase with specific inhibitors as a strategy in cancer therapy. *Cell. Mol. Life Sci.* **2010**, *67* (21), 3663−3681.
(10) Kaina, B.; Christmann, M. DNA repair in personalized brain cancer therapy with Temozolomide and nitrosoureas. *DNA Repair* **2019**, *78*, 128−141.
(11) Gerson, S. L. MGMT: Its role in cancer aetiology and cancer therapeutics. *Nat. Rev. Cancer* **2004**, *4* (4), 296−307.
(12) Pegg, A. E. Multifaceted roles of alkyltransferase and related proteins in DNA repair, DNA damage, resistance to chemotherapy, and research tools. *Chem. Res. Toxicol.* **2011**, *24* (5), 618−639.
(13) Sun, G. H.; Zhao, L. J.; Zhong, R. G.; Peng, Y. Z. The specific role of O-6-methylguanine-DNA methyltransferase inhibitors in cancer chemotherapy. *Future Med. Chem.* **2018**, *10* (16), 1971−1996.
(14) Sun, G. H.; Fan, T. J.; Zhang, N.; Ren, T.; Zhao, L. J.; Zhong, R. G. Identification of the structural features of guanine derivatives as MGMT inhibitors using 3D-QSAR modeling combined with molecular docking. *Molecules* **2016**, *21* (7), 823.
(15) Sun, G. H.; Fan, T. J.; Sun, X. D.; Hao, Y. X.; Cui, X.; Zhao, L. J.; Ren, T.; Zhou, Y.; Zhong, R. G.; Peng, Y. Z. In silico prediction of O-6-methylguanine-DNA methyltransferase inhibitory potency of base analogs with QSAR and machine learning methods. *Molecules* **2018**, *23* (11), 2892.
(16) Middleton, M. R.; Margison, G. P. Improvement of chemotherapy efficacy by inactivation of a DNA-repair pathway. *Lancet Oncol.* **2003**, *4* (1), 37−44.
(17) Ranson, M.; Middleton, M. R.; Bridgewater, J.; Lee, S. M.; Dawson, M.; Jowle, D.; Halbert, G.; Waller, S.; McGrath, H.; Gumbrell, L.; McElhinney, R. S.; Donnelly, D.; McMurry, T. B. H.; Margison, G. P. L. Lomeguatrib, a Potent Inhibitor of *O*6-Alkylguanine-DNA-Alkyltransferase: Phase I Safety, Pharmacodynamic, and Pharmacokinetic Trial and Evaluation in Combination with Temozolomide in Patients with Advanced Solid Tumors. *Clin. Cancer Res.* **2006**, *12* (5), 1577−1584.
(18) Warren, K. E.; Gururangan, S.; Geyer, J. R.; McLendon, R. E.; Poussaint, T. Y.; Wallace, D.; Balis, F. M.; Berg, S. L.; Packer, R. J.; Goldman, S.; Minturn, J. E.; Pollack, I. F.; Boyett, J. M.; Kun, L. E. A phase II study of O6-benzylguanine and Temozolomide in pediatric patients with recurrent or progressive high-grade gliomas and brainstem gliomas: a Pediatric Brain Tumor Consortium study. *J. Neuro Oncol.* **2012**, *106* (3), 643−649.
(19) Yoshida, T.; Shimizu, K.; Ushio, Y.; Hayakawa, T.; Mogami, H.; Sakamoto, Y. The mechanism and overcoming of resistance in ACNU-resistant sublines of C6 and 9L rat glioma. *J. Neuro Oncol.* **1987**, *5* (3), 195−203.
(20) Fletcher, J. I.; Haber, M.; Henderson, M. J.; Norris, M. D. ABC transporters in cancer: more than just drug efflux pumps. *Nat. Rev. Cancer* **2010**, *10* (2), 147−156.
(21) Potęga, A. Glutathione-mediated conjugation of anticancer drugs: An overview of reaction mechanisms and biological significance for drug detoxification and bioactivation. *Molecules* **2022**, *27* (16), 5252.
(22) Berhane, K.; Hao, X. Y.; Egyhazi, S.; Hansson, J.; Ringborg, U.; Mannervik, B. Contribution of glutathione transferase M3−3 to 1,3-bis(2-chloroethyl)-1-nitrosourea resistance in a human nonsmall cell lung-cancer cell-line. *Cancer Res.* **1993**, *53* (18), 4257−4261.
(23) Fan, T. J.; Sun, G. H.; Sun, X. D.; Zhao, L. J.; Zhong, R. G.; Peng, Y. Z. Tumor energy metabolism and potential of 3-bromopyruvate as an inhibitor of aerobic glycolysis: implications in tumor treatment. *Cancers* **2019**, *11* (3), 317.
(24) Vander Heiden, M. G.; Cantley, L. C.; Thompson, C. B. Understanding the Warburg effect: the metabolic requirements of cell proliferation. *Science* **2009**, *324* (5930), 1029−1033.
(25) Hanahan, D.; Weinberg, R. A. Hallmarks of cancer: The next generation. *Cell* **2011**, *144* (5), 646−674.
(26) Lin, J. G.; Xia, L. Z.; Liang, J. X.; Han, Y. Q.; Wang, H. R.; Oyang, L. D.; Tan, S. M.; Tian, Y. T.; Rao, S.; Chen, X. Y.; Tang, Y. Y.; Su, M.; Luo, X.; Wang, Y.; Wang, H.; Zhou, Y. J.; Liao, Q. J. The roles of glucose metabolic reprogramming in chemo- and radioresistance. *J. Exp. Clin. Cancer Res.* **2019**, *38*, 218.
(27) Varghese, E.; Samuel, S. M.; Líšková, A.; Samec, M.; Kubatka, P.; Büsselberg, D. Targeting glucose metabolism to overcome resistance to anticancer chemotherapy in breast cancer. *Cancers* **2020**, *12* (8), 2252.
(28) Davidescu, M.; Macchioni, L.; Scaramozzino, G.; Cristina Marchetti, M.; Migliorati, G.; Vitale, R.; Corcelli, A.; Roberti, R.; Castigli, E.; Corazzi, L. The energy blockers bromopyruvate and lonidamine lead GL15 glioblastoma cells to death by different p53-dependent routes. *Sci. Rep.* **2015**, *5*, 14343.
(29) Huang, Y. X.; Sun, G. H.; Sun, X. D.; Li, F. F.; Zhao, L. J.; Zhong, R. G.; Peng, Y. Z. The potential of lonidamine in combination with chemotherapy and physical therapy in cancer treatment. *Cancers* **2020**, *12* (11), 3332.
(30) Laussel, C.; Léon, S. Cellular toxicity of the metabolic inhibitor 2-deoxyglucose and associated resistance mechanisms. *Biochem. Pharmacol.* **2020**, *182*, 114213.
(31) Sun, X. D.; Sun, G. H.; Huang, Y. X.; Hao, Y. X.; Tang, X. Y.; Zhang, N.; Zhao, L. J.; Zhong, R. G.; Peng, Y. Z. 3-Bromopyruvate regulates the status of glycolysis and BCNU sensitivity in human hepatocellular carcinoma cells. *Biochem. Pharmacol.* **2020**, *177*, 113988.
(32) Sun, X. D.; Sun, G. H.; Huang, Y. X.; Zhang, S. F.; Tang, X. Y.; Zhang, N.; Zhao, L. J.; Zhong, R. G.; Peng, Y. Z. Glycolytic inhibition by 3-bromopyruvate increases the cytotoxic effects of chloroethylnitrosoureas to human glioma cells and the DNA interstrand cross-links formation. *Toxicology* **2020**, *435*, 152413.
(33) Sun, X.; Fan, T.; Sun, G.; Zhou, Y.; Huang, Y.; Zhang, N.; Zhao, L.; Zhong, R.; Peng, Y. 2-Deoxy-D-glucose increases the sensitivity of glioblastoma cells to BCNU through the regulation of glycolysis, ROS and ERS pathways: In vitro and in vivo validation. *Biochem. Pharmacol.* **2022**, *199*, 115029.
(34) Cioli, V.; Bellocci, B.; Putzolu, S.; Malorni, W.; Demartino, C. Anti-spermogenic activity of lonidamine (AF-1890) in rabbit. *Ultramicroscopy* **1980**, *5* (3), 418.
(35) Ben-Yoseph, O.; Lyons, J. C.; Song, C. W.; Ross, B. D. Mechanism of action of lonidamine in the 9L brain tumor model involves inhibition of lactate efflux and intracellular acidification. *J. Neuro Oncol.* **1998**, *36* (2), 149−157.
(36) Nath, K.; Nelson, D. S.; Ho, A. M.; Lee, S. C.; Darpolor, M. M.; Pickup, S.; Zhou, R.; Heitjan, D. F.; Leeper, D. B.; Glickson, J. D. $^{31}$P


https://doi.org/10.1021/acsomega.4c00641
*ACS Omega* 2024, 9, 36134−36147

and $^{1}$H MRS of DB-1 melanoma xenografts: lonidamine selectively decreases tumor intracellular pH and energy status and sensitizes tumors to melphalan. *NMR Biomed.* **2013**, *26* (1), 98−105.
(37) Nath, K.; Guo, L. L.; Nancolas, B.; Nelson, D. S.; Shestov, A. A.; Lee, S. C.; Roman, J.; Zhou, R.; Leeper, D. B.; Halestrap, A. P.; Blair, I. A.; Glickson, J. D. Mechanism of antineoplastic activity of lonidamine. *Biochim. Biophys. Acta Rev. Cancer* **2016**, *1866* (2), 151−162.
(38) Nath, K.; Nelson, D. S.; Putt, M. E.; Leeper, D. B.; Garman, B.; Nathanson, K. L.; Glickson, J. D. Comparison of the lonidamine potentiated effect of nitrogen mustard alkylating agents on the systemic treatment of DB-1 human melanoma xenografts in mice. *PLoS One* **2016**, *11* (6), No. e0157125.
(39) Nath, K.; Nelson, D. S.; Heitjan, D. F.; Leeper, D. B.; Zhou, R.; Glickson, J. D. Lonidamine induces intracellular tumor acidification and ATP depletion in breast, prostate and ovarian cancer xenografts and potentiates response to doxorubicin. *NMR Biomed.* **2015**, *28* (3), 281−290.
(40) Nath, K.; Roman, J.; Nelson, D. S.; Guo, L. L.; Lee, S. C.; Orlovskiy, S.; Muriuki, K.; Heitjan, D. F.; Pickup, S.; Leeper, D. B.; Blair, I. A.; Putt, M. E.; Glickson, J. D. Effect of differences in metabolic activity of melanoma models on response to lonidamine plus doxorubicin. *Sci. Rep.* **2018**, *8*, 14654.
(41) Nath, K.; Nelson, D. S.; Roman, J.; Putt, M. E.; Lee, S. C.; Leeper, D. B.; Glickson, J. D. Effect of lonidamine on systemic therapy of DB-1 human melanoma xenografts with Temozolomide. *Anticancer Res.* **2017**, *37* (7), 3413−3421.
(42) Huang, Y.; Wang, P.; Fan, T.; Zhang, N.; Zhao, L.; Zhong, R.; Sun, G. Energy blocker lonidamine reverses nimustine resistance in human glioblastoma cells through energy blockade, redox homeostasis disruption, and O6-methylguanine-DNA methyltransferase down-regulation: in vitro and in vivo validation. *ACS Pharmacol. Transl. Sci.* **2024**, *7* (5), 1518−1532.
(43) Berridge, M. V.; Tan, A. S. Characterization of the cellular reduction of 3-(4,5-dimethylthiazol-2-yl)-2,5-diphenyltetrazolium bromide (MTT) - subcellular-localization, substrate dependence, and involvement of mitochondrial electron-transport in MTT reduction. *Arch. Biochem. Biophys.* **1993**, *303* (2), 474−482.
(44) Jin, Z. J. About the evaluation of drug combination. *Acta Pharmacol. Sin.* **2004**, *25* (2), 146−147.
(45) Smith, P. K.; Krohn, R. I.; Hermanson, G. T.; Mallia, A. K.; Gartner, F. H.; Provenzano, M. D.; Fujimoto, E. K.; Goeke, N. M.; Olson, B. J.; Klenk, D. C. Measurement of protein using bicinchoninic acid. *Anal. Biochem.* **1985**, *150* (1), 76−85.
(46) Ellman, G. L. Tissue sulfhydryl groups. *Arch. Biochem. Biophys.* **1959**, *82* (1), 70−77.
(47) Lebel, C. P.; Ischiropoulos, H.; Bondy, S. C. Evaluation of the probe 2',7'-dichlorofluorescin as an indicator of reactive oxygen species formation and oxidative stress. *Chem. Res. Toxicol.* **1992**, *5* (2), 227−231.
(48) Smiley, S. T.; Reers, M.; Mottolahartshorn, C.; Lin, M.; Chen, A.; Smith, T. W.; Steele, G. D.; Chen, L. B. Intracellular heterogeneity in mitochondrial-membrane potentials revealed by a J-aggregate-forming lipophilic cation JC-1. *Proc. Natl. Acad. Sci. U.S.A.* **1991**, *88* (9), 3671−3675.
(49) Spanswick, V. J.; Hartley, J. M.; Hartley, J. A. Measurement of DNA interstrand crosslinking in individual cells using the single cell gel electrophoresis (Comet) assay. In *Drug-DNA Interaction Protocols*; Fox, K. R., Ed.; Humana Press: Totowa, NJ, 2010; pp 267−282.
(50) Le, P. M.; Silvestri, V. L.; Redstone, S. C.; Dunn, J. B.; Millard, J. T. Cross-linking by epichlorohydrin and diepoxybutane correlates with cytotoxicity and leads to apoptosis in human leukemia (HL-60) cells. *Toxicol. Appl. Pharmacol.* **2018**, *352*, 19−27.
(51) Scatena, R.; Bottoni, P.; Pontoglio, A.; Mastrototaro, L.; Giardina, B. Glycolytic enzyme inhibitors in cancer treatment. *Expert Opin. Invest. Drugs* **2008**, *17* (10), 1533−1545.
(52) Granchi, C.; Minutolo, F. Anticancer agents that counteract tumor glycolysis. *ChemMedChem* **2012**, *7* (8), 1318−1350.
(53) Guo, L. L.; Shestov, A. A.; Worth, A. J.; Nath, K.; Nelson, D. S.; Leeper, D. B.; Glickson, J. D.; Blair, I. A. Inhibition of Mitochondrial Complex II by the Anticancer Agent Lonidamine. *J. Biol. Chem.* **2016**, *291* (1), 42−57.
(54) Cheng, G.; Zhang, Q.; Pan, J.; Lee, Y.; Ouari, O.; Hardy, M.; Zielonka, M.; Myers, C. R.; Zielonka, J.; Weh, K.; Chang, A. C.; Chen, G. A.; Kresty, L.; Kalyanaraman, B.; You, M. Targeting lonidamine to mitochondria mitigates lung tumorigenesis and brain metastasis. *Nat. Commun.* **2019**, *10*, 2205.
(55) Ihrlund, L. S.; Hernlund, E.; Khan, O.; Shoshan, M. C. 3-Bromopyruvate as inhibitor of tumour cell energy metabolism and chemopotentiator of platinum drugs. *Mol. Oncol.* **2008**, *2* (1), 94−101.
(56) Yankovskaya, V.; Horsefield, R.; Törnroth, S.; Luna-Chavez, C.; Miyoshi, H.; Léger, C.; Byrne, B.; Cecchini, G.; Iwata, S. Architecture of succinate dehydrogenase and reactive oxygen species generation. *Science* **2003**, *299* (5607), 700−704.
(57) Davis, M. R.; Baillie, T. A. Studies on the formation of reactive intermediates from the antineoplastic agent n,n'-bis(2-chloroethyl)-n-nitrosourea (BCNU) in-vitro and in-vivo - characterization of novel glutathione adducts by ionspray tandem mass-spectrometry. *J. Mass Spectrom.* **1995**, *30* (1), 57−68.
(58) Moloney, J. N.; Cotter, T. G. ROS signalling in the biology of cancer. *Semin. Cell Dev. Biol.* **2018**, *80*, 50−64.
(59) Nancolas, B.; Guo, L. L.; Zhou, R.; Nath, K.; Nelson, D. S.; Leeper, D. B.; Blair, I. A.; Glickson, J. D.; Halestrap, A. P. The anti-tumour agent lonidamine is a potent inhibitor of the mitochondrial pyruvate carrier and plasma membrane monocarboxylate transporters. *Biochem. J.* **2016**, *473*, 929−936.
(60) Bai, P.; Fan, T.; Sun, G.; Wang, X.; Zhao, L.; Zhong, R. The dual role of DNA repair protein MGMT in cancer prevention and treatment. *DNA Repair* **2023**, *123*, 103449.
(61) Bai, P.; Fan, T.; Wang, X.; Zhao, L.; Zhong, R.; Sun, G. Modulating MGMT expression through interfering with cell signaling pathways. *Biochem. Pharmacol.* **2023**, *215*, 115726.
(62) Sun, G. H.; Zhang, N.; Zhao, L. J.; Fan, T. J.; Zhang, S. F.; Zhong, R. G. Synthesis and antitumor activity evaluation of a novel combi-nitrosourea prodrug: Designed to release a DNA cross-linking agent and an inhibitor of O-6-alkylguanine-DNA alkyltransferase. *Bioorg. Med. Chem.* **2016**, *24* (9), 2097−2107.


https://doi.org/10.1021/acsomega.4c00641
*ACS Omega* 2024, 9, 36134−36147